Hyperfine energy levels of alkali-metal dimers: Ground-state polar molecules in electric and magnetic fields

J. Aldegunde,* Ben A. Rivington, Piotr S. Żuchowski,† and Jeremy M. Hutson‡
Department of Chemistry, Durham University, South Road, Durham DH1 3LE, United Kingdom
(Received 12 July 2008; published 30 September 2008)

We investigate the energy levels of heteronuclear alkali-metal dimers in levels correlating with the lowest rotational level of the ground electronic state, which are important in efforts to produce ground-state ultracold molecules. We use density-functional theory to calculate nuclear quadrupole and magnetic coupling constants for KRb and RbCs and explore the hyperfine structure in the presence of electric and magnetic fields. For nonrotating states, the zero-field splittings are dominated by the electron-mediated part of the nuclear spin-spin coupling. They are a few kilohertz for KRb isotopologs and a few tens of kilohertz for RbCs isotopologs.

DOI: 10.1103/PhysRevA.78.033434 PACS number(s): 37.10.Pq, 31.15.aj, 33.15.Pw

I. INTRODUCTION

There is great interest in the formation of ultracold molecules and in achieving molecular Bose-Einstein condensation and Fermi degeneracy. Molecules can be formed in ultracold atomic gases either by photoassociation [1,2] or by tuning through zero-energy Feshbach resonances with magnetic fields [1,3]. Since alkali-metal atoms are easier to cool than other species, most work on ultracold molecule formation has focused on alkali-metal dimers.

There is particular interest in forming ultracold *polar* molecules. Dipole-dipole interactions are both stronger and longer-range than the quadrupole-quadrupole and dispersion forces that exist between nonpolar molecules. As a result, dipolar quantum gases are predicted to have novel properties [4]. Ultracold dipolar molecules might also be used in quantum-information storage and processing [5].

Both photoassociation and Feshbach resonance tuning form molecules that are initially in highly excited vibrational states. Quantum gases of such molecules can be formed [6–8], but they are long-lived only in very specific cases, such as homonuclear fermion dimers in the highest vibrational level, tuned to large scattering lengths [9]. For other cases the molecules undergo fast inelastic collisions that lead to trap loss [10–12]. Furthermore, even heteronuclear molecules are essentially nonpolar when they are in weakly bound vibrational states. Because of this, there is intense current effort directed at producing ultracold molecules in their absolute ground states, for which inelastic losses cannot occur and for which heteronuclear molecules have significant dipole moments. Very recently, there have been major advances in transferring Feshbach molecules to deeply bound states by laser-based methods such as stimulated Raman adiabatic passage [13–15]. Formation of quantum gases of ground-state molecules is now within reach.

There has been a considerable amount of work on the energy levels of homonuclear alkali metal dimers, especially in the near-dissociation states formed by Feshbach resonance tuning [16–19]. However, remarkably little is known about the hyperfine structure of the energy levels of alkali-metal dimers in their lowest rotational states. The tiny splittings are beyond the resolution of most spectroscopic techniques. Nevertheless, an understanding of these energy levels is essential in designing laser-based methods to produce molecules in specific states and will be crucial in developing methods to control the resulting quantum gases. The purpose of the present paper is to investigate the lowest energy levels of heteronuclear alkali-metal dimers and to explore how they behave in electric and magnetic fields. We focus here on KRb and RbCs, which are topical for current experiments.

II. THEORY

Molecular Hamiltonian

The Hamiltonian of a diatomic molecule in the presence of external magnetic and electric fields can be decomposed into six different contributions: the electronic, vibrational, rotational, hyperfine, Stark, and Zeeman terms. By restricting our analysis to $^1\Sigma$ molecules in the ground electronic state and in a fixed vibrational level, the first two terms take a constant value and the rotational, hyperfine, Stark, and Zeeman parts of the Hamiltonian can be written [20–22]

$$H = H_{\mathrm{rot}} + H_{\mathrm{hf}} + H_{\mathrm{S}} + H_{\mathrm{Z}}, \tag{1}$$

where

$$H_{\mathrm{rot}} = B_v \boldsymbol{N}^2 - D_v \boldsymbol{N}^2 \boldsymbol{N}^2, \tag{2}$$

$$H_{\mathrm{hf}} = \sum_{i=1}^{2} \boldsymbol{V}_i \cdot \boldsymbol{Q}_i + \sum_{i=1}^{2} c_i \boldsymbol{N} \cdot \boldsymbol{I}_i + c_3 \boldsymbol{I}_1 \cdot \boldsymbol{T} \cdot \boldsymbol{I}_2 + c_4 \boldsymbol{I}_1 \cdot \boldsymbol{I}_2, \tag{3}$$

$$H_{\mathrm{S}} = -\boldsymbol{\mu} \cdot \boldsymbol{E}, \tag{4}$$

$$H_{\mathrm{Z}} = -g_r \mu_N \boldsymbol{N} \cdot \boldsymbol{B} - \sum_{i=1}^{2} g_i \mu_N \boldsymbol{I}_i \cdot \boldsymbol{B}(1 - \sigma_i). \tag{5}$$

The three different sources of angular momentum in a $^1\Sigma$ diatomic molecule are the rotational angular momentum $\boldsymbol{N}$ and the spins $\boldsymbol{I}_1$ and $\boldsymbol{I}_2$ of nuclei 1 and 2. The rotational and

*Jesus.Aldegunde@durham.ac.uk
†Piotr.Zuchowski@durham.ac.uk
‡J.M.Hutson@durham.ac.uk

centrifugal distortion constants of the molecule are B_v and D_v (the centrifugal distortion contribution will not be considered in the calculations). The hyperfine Hamiltonian of Eq. (3) consists of four terms. The first is the electric quadrupole interaction with coupling constants $(eqQ)_1$ and $(eqQ)_2$, where q_i is the electric field gradient at nucleus i and eQ_i is its nuclear quadrupole moment. The second is the interaction between the nuclear magnetic moments and the magnetic field created by the rotation of the molecule, with spin-rotation coupling constants c_1 and c_2. The two remaining terms represent the tensor and scalar interactions between the nuclear dipole moments, with spin-spin coupling constants c_3 and c_4, respectively. The tensor $\boldsymbol{T}$ describes the angle dependence of the direct spin-spin interaction and the anisotropic part of the indirect spin-spin interaction [22].

The Stark and Zeeman Hamiltonians, Eqs. (4) and (5), describe the interaction of the molecule with an external electric field $\boldsymbol{E}$ and magnetic field $\boldsymbol{B}$, where $\boldsymbol{\mu}$ is the molecular dipole moment. The Zeeman Hamiltonian consists of two terms representing the rotational and nuclear Zeeman effects. The former arises because the molecular rotation produces a magnetic moment $g_r\mu_N\boldsymbol{N}$, where g_r is the rotational g factor of the molecule, which interacts with the external magnetic field. The latter arises from the interaction of the nuclear magnetic moments $g_i\mu_N\boldsymbol{I}_i$ with the magnetic field, where g_i is the nuclear g factor for nucleus i and $\boldsymbol{I}_i$ is its nuclear spin. The nuclear shielding tensor $\boldsymbol{\sigma}_i$ is approximated here by its isotropic part σ_i; terms involving the anisotropy of $\boldsymbol{\sigma}_i$ are extremely small for the states considered here. The diamagnetic Zeeman effect is not included in the Hamiltonian as it causes level splittings of less than 1 Hz for the range of magnetic fields considered in this work.

The nuclear g factors and quadrupole moments are well known [23]. The dipole moments of KRb and RbCs have been calculated from relativistic electronic structure calculations [24,25].

III. EVALUATION OF THE COUPLING CONSTANTS

Nuclear quadrupole coupling constants have been measured for several alkali metal dimers as shown in Table I. However, the only such species for which the magnetic coupling constants have been measured is Na_2 [26], and even there the experiments did not resolve hyperfine splittings for the $N=0$ state. To the best of our knowledge, no experimental data are available for the hyperfine structure of the molecules we consider here, KRb and RbCs, in their ground electronic state. We therefore carry out electronic structure calculations to estimate them, using density-functional theory (DFT). The electric quadrupole coupling constants $(eqQ)_1$ and $(eqQ)_2$ are directly related to electron densities, while the nuclear shielding tensors and spin-spin coupling constants c_3 and c_4 can be expressed as second derivatives of the electronic energy [36]. The spin-rotation constants c_1 and c_2 are related to the nuclear shielding tensor. In the present work we use the Amsterdam density functional (ADF) package [37,38], which uses Slater functions and allows the inclusion of relativistic corrections. The rotational g factor (not implemented in the ADF code) is evaluated with the DALTON package [39].

TABLE I. Comparison of electric quadrupole coupling constants for alkali-metal atoms calculated as described in the text with experimental values. The units are megahertz.

Molecule	$(eQq)^{\text{calc}}$	$(eQq)^{\text{expt}}$	Reference
$^{23}Na_2$	−0.456	−0.459	[26]
$^{39}K_2$	−0.290	−0.158	[27]
$^{39}K^{19}F$	−7.87	−7.93	[28]
$^{39}K^{7}Li$	−0.830	−1.03	[29]
$^{39}K^{23}Na$	−0.671	−0.718	[29] (for K)
$^{39}K^{23}Na$	−0.216	0.171[a]	[29] (for Na)
$^{85}Rb_2$	−2.457	−1.1	[27]
$^{85}Rb^{19}F$	−73.1	−70.7	[30]
$^{85}Rb^{35}Cl$	−53.5	−52.8	[31]
$^{85}Rb^{79}Br$	−46.8	−47.2	[32]
$^{85}Rb^{127}I$	−39.6	−58.9	[33]
$^{85}Rb^{7}Li$	−8.04	−9.12	[29]
$^{133}Cs^{19}F$	1.30	1.25	[34]
$^{133}Cs^{35}Cl$	1.05	$\leqslant$1.1[a]	[35]

[a]Only the absolute value was determined experimentally.

The objective of the present paper is to explore the behavior of the molecular energy levels in the presence of external fields. A detailed discussion of the features and effectiveness of the many different methods and basis sets available for the calculation of the coupling constants is beyond the scope of this work. However, to estimate the reliability of the functionals and basis sets employed here we compare the coupling constants obtained for a group of molecules containing alkali-metal atoms with experimental results in Tables I–IV. For simplicity we have omitted experimental uncertainties and vibrational state dependences. It may be seen that the calculated coupling constants are generally within 40% of the experimental values, except in occasional cases where the experimental values are unusually small (such as c_4 for $^{85}Rb^{35}Cl$).

Evaluation of hyperfine coupling constants requires a basis set that properly describes the electron density near the nuclei. Because of this, we employ all-electron basis sets rather than valence basis sets with effective core potentials. However, for core orbitals of heavy elements such as those considered here, relativistic effects can be important. In the

TABLE II. Comparison between spin-rotation coupling constants calculated as described in the text and experimentally measured. The label 1 refers to the less electronegative atom (K, Rb, or Cs) and the label 2 to the more electronegative one. The units are kilohertz.

Molecule	c_1^{calc}	c_1^{expt}	c_2^{calc}	c_2^{expt}	Reference
$^{23}Na_2$	0.299	0.243	0.299	0.243	[26]
$^{39}K^{19}F$	0.235	0.270	17.5	10.7	[28]
$^{85}Rb^{19}F$	0.598	0.498	16.1	10.6	[30]
$^{35}Rb^{35}Cl$	0.457	0.395	0.569	0.394	[31]
$^{133}Cs^{19}F$	1.05	0.662	21.9	15.1	[34]

TABLE III. Comparison between spin-spin coupling constants calculated as described in the text and experimentally measured. The units are kilohertz.

Molecule	c_3^{calc}	c_3^{expt}	c_4^{calc}	c_4^{expt}	Reference
$^{23}Na_2$	0.298	0.303	1.358	1.067	[26]
$^{39}K^{19}F$	0.470	0.540	0.032	0.030	[28]
$^{85}Rb^{19}F$	0.751	0.797	0.151	0.237	[30]
$^{85}Rb^{35}Cl$	0.027	0.033	0.010	0.026	[31]
$^{133}Cs^{19}F$	0.875	0.927	0.471	0.627	[34]

present work, relativistic corrections were included by means of, the two-component zero-order regular approximation [42–44], including spin-orbit coupling as well as scalar effects (which are the equivalent of Darwin and mass-velocity terms in the Breit-Pauli Hamiltonian).

DFT generally performs well for calculations of electric quadrupole coupling constants for main-group elements [45–53]. Following most of these examples, we use the Becke three-parameter Lee-Yang-Parr hybrid (B3LYP) functional [54,55] in our calculations with the QZ4P basis set (a quadruple-ζ all-electron basis set with four polarization functions).

Shielding tensors were evaluated using the Keal-Tozer (KT2) functional [56] with the same basis set and relativistic correction as for the quadrupole coupling constants. For calculation of shielding tensors of main-group atoms (H, C, N, O, and F), the performance of this functional is excellent, and is better [57] than that of more popular functionals such as the Becke–Lee-Yang-Parr (BLYP) [54,58] and B3LYP functionals.

Two nuclear magnetic moments can interact both directly (through space) and indirectly (via the electron distribution). The coupling constant for the direct interaction is [22,59]

$$R_{\text{DD}} = \frac{\mu_0}{4\pi}\frac{\mu_N^2}{h} g_1 g_2 \langle R^{-3} \rangle, \tag{6}$$

where R is the internuclear distance. The indirect interaction is represented by a tensor $\boldsymbol{J}$ [22,59] with isotropic part J_{iso} and anisotropy $\Delta J = J_{\parallel} - J_{\perp}$. The coupling constants c_3 and c_4 are related to the direct and indirect components by [22,59]

$$c_3 = R_{\text{DD}} - \frac{\Delta J}{3} \tag{7}$$

and

$$c_4 = J_{\text{iso}}. \tag{8}$$

In the present work, $\langle R^{-3} \rangle$ was approximated by R_e^{-3}, where R_e is the equilibrium distance.

Methods for calculating spin-spin coupling constants have been recently reviewed by Helgaker *et al.* [60]. In the present work, the components of $\boldsymbol{J}$ were calculated using the same methods as for the quadrupole coupling constants, except that the Perdew-Burke-Ernzerhof (PBE) [61] functional was used. This functional produced results slightly closer to the experimental measurements than KT2 for the molecules considered in Table III (although the differences were small). The BLYP functional performed well for all except Na_2, for which it gave the wrong sign and order of magnitude; it also gave qualitatively different results from the PBE and KT2 functionals for KRb and RbCs.

TABLE IV. Comparison between rotational g factors calculated as described in the text and experimentally measured.

Molecule	g_r^{calc}	g_r^{expt}	Reference
$^{23}Na_2$	0.0324	0.0386	[40]
$^{39}K_2$	0.0247	0.0212	[40]
$^{23}Na^{39}K$	0.0253	0.0253	[41]
$^{85}Rb_2$	0.0082	0.0095	[40]
$^{133}Cs_2$	0.0051	0.0054	[40]

ADF does not calculate spin-rotation constants directly. However, the spin-rotation constants are given approximately by [62–64]

$$c_i \approx \frac{2m_e B_v g_i}{m_p}(\sigma_{i\parallel} - \sigma_{i\perp}) \quad \text{for } i = 1,2, \tag{9}$$

where m_p and m_e are the proton and electron masses, B_v is the rotational constant, g_i is the nuclear g factor, and $\sigma_{i\parallel} - \sigma_{i\perp}$ is the anisotropy of the nuclear shielding tensor $\boldsymbol{\sigma}_i$. Two approximations underlie this expression. First, a quadrupole term has been neglected. Second, it was obtained in the frame of the nonrelativistic theory developed by Flygare [62]. However, previous studies [65] and our own results (see Table II) suggest that it can be applied reliably in the relativistic case.

Lastly, the rotational g factors were evaluated with the DALTON program using the KT2 functional and the all-electron basis sets of Huzinaga and co-workers [66,67]. Again, the choice of the functional is based on its reliability for this molecular property [68]. No relativistic corrections were included in this case. Previous calculations [69] for hydrogen halides and noble gas hydride cations including atoms as heavy as I and Xe suggest that relativistic corrections are relatively small for rotational g factors (less than 5% of the nonrelativistic value).

The coupling constants obtained for KRb and RbCs are given in Tables V and VI. All the calculations were carried out at the equilibrium geometries, R_e=4.07 Å for KRb [70] and 4.37 Å for RbCs [71]. This neglects small corrections due to vibrational averaging even for v=0, but nevertheless gives results that are qualitatively valid for any low-lying vibrational state. ADF generally gives coupling constants for only one isotopic species, but the others may be obtained by simple scaling. The nuclear quadrupole coupling constants scale with the nuclear quadrupoles Q_i, the spin-spin coupling constants with the product of nuclear g factors $g_i g_j$, and the spin-rotation coupling constant with the product of g_i and the rotational constant B_v. The rotational g factor scales in a more complicated way that depends on B_v and the shift of the center of mass [72].

TABLE V. Nuclear properties and coupling constants for the different isotopic species of the KRb molecule.

	$^{39}K^{85}Rb$	$^{39}K^{87}Rb$	$^{40}K^{85}Rb$	$^{40}K^{87}Rb$	$^{41}K^{85}Rb$	$^{41}K^{87}Rb$
I_K	3/2	3/2	4	4	3/2	3/2
I_{Rb}	5/2	3/2	5/2	3/2	5/2	3/2
g_K	0.261	0.261	−0.324	−0.324	0.143	0.143
g_{Rb}	0.541	1.834	0.541	1.834	0.541	1.834
B_v (GHz)	1.142	1.134	1.123	1.114	1.104	1.096
$(eQq)_K$ (MHz)	−0.245	−0.245	0.306	0.306	−0.298	−0.298
$(eQq)_{Rb}$ (MHz)	−3.142	−1.520	−3.142	−1.520	−3.142	−1.520
σ_K (ppm)	1321	1321	1321	1321	1321	1321
σ_{Rb} (ppm)	3469	3469	3469	3469	3469	3469
c_K (Hz)	19.9	19.8	−24.2	−24.1	10.5	10.4
c_{Rb} (Hz)	127.0	427.5	124.8	420.1	122.8	413.1
c_3 (Hz)	11.5	38.9	−14.2	−48.2	6.3	21.3
c_4 (Hz)	482.5	1635.7	−599.0	−2030.4	264.3	896.2
g_r	0.0144	0.0142	0.0141	0.0140	0.0139	0.0138
μ (D)	0.76	0.76	0.76	0.76	0.76	0.76

IV. HYPERFINE ENERGY LEVELS

We calculate the hyperfine levels by diagonalizing the complete Hamiltonian of Eqs. (2)–(5) in a basis set of angular momentum functions. We employ three different basis sets,

$$|I_1 M_1 I_2 M_2 N M_N\rangle \quad \text{(uncoupled basis)}, \tag{10}$$

$$|(I_1 I_2) I M_I N M_N\rangle \quad \text{(spin-coupled basis)}, \tag{11}$$

$$|(I_1 I_2) I N F M_F\rangle \quad \text{(fully coupled basis)}. \tag{12}$$

Here I and F are quantum numbers for the total nuclear spin and total angular momentum and M_I and M_F represent their projections onto the Z axis defined by the external field. We consider here only cases in which only one field, electric or magnetic, is present. The matrix elements corresponding to the different terms of the Hamiltonian in each of the basis sets are calculated through standard angular momentum techniques [73].

The use of three basis sets rather than one helps in assigning quantum numbers to the energy levels. Although the Hamiltonian matrix is not diagonal in any of the basis sets employed, it is usually closer to diagonal for one basis than for the others. When one coefficient of an eigenvector is much larger than the others, it is possible to assign approximate quantum numbers to the state concerned. However, different basis sets achieve this in different field regimes.

TABLE VI. Nuclear properties and coupling constants for the different isotopic species of the RbCs molecule.

	$^{85}Rb^{133}Cs$	$^{87}Rb^{133}Cs$
I_{Rb}	5/2	3/2
I_{Cs}	7/2	7/2
g_{Rb}	0.541	1.834
g_{Cs}	0.738	0.738
B_v (GHz)	0.511	0.504
$(eQq)_{Rb}$ (MHz)	−1.803	−0.872
$(eQq)_{Cs}$ (MHz)	0.051	0.051
σ_{Rb} (ppm)	3531	3531
σ_{Cs} (ppm)	6367	6367
c_{Rb} (Hz)	29.4	98.4
c_{Cs} (Hz)	196.8	194.1
c_3 (Hz)	56.8	192.4
c_4 (Hz)	5116.6	17345.4
g_r	0.0063	0.0062
μ	1.25	1.25

A. Zeeman splitting for rotational ground-state molecules ($N=0$)

Figure 1 shows the Zeeman splittings for energy levels of $^{39}K^{85}Rb$ with $N=0$. The splittings are dominated by the scalar nuclear spin-spin interaction and the nuclear Zeeman effect, which are the only terms in the Hamiltonian with matrix elements diagonal in N for $N=0$. It should be noted that the scalar spin-spin coupling is entirely mediated by the electron distribution, and has no contribution from the direct dipolar interaction. In the absence of external fields, the energy levels are split into groups labeled by the total nuclear spin I. For small magnetic fields B, I remains a nearly good quantum number and the levels split according to the value of its projection M_I (which in this case coincides with the projection of the total angular momentum, which is always a good quantum number). Energy levels corresponding to the same value of M_I display avoided crossings as a function of the field as shown in Fig. 2. For fields well above the crossings (which are at 2–10 G in this case), I is destroyed and the good quantum numbers are M_{Rb} and M_K. Since both nuclear g factors are positive for $^{39}K^{85}Rb$, states where both projec-

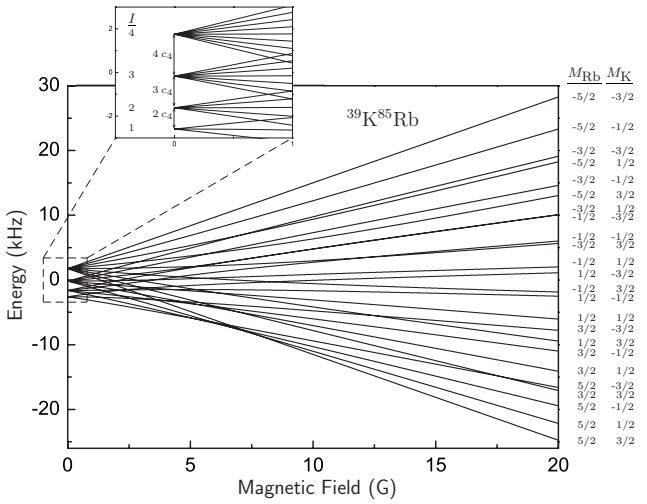

FIG. 1. Zeeman levels for ^{39}K^{85}Rb(v=0,N=0).

tions are positive are high-field-seeking and those where both are negative are low-field-seeking.

Although the splittings at low fields are dominated by the scalar spin-spin coupling, there are several terms in the Hamiltonian that are off-diagonal in N. The energies are therefore obtained by diagonalizing a full matrix that includes enough rotational levels for convergence. For the Zeeman effect, the only off-diagonal terms involving N=0 are the electric quadrupole coupling and the tensor spin-spin coupling, both of which are small. Convergence for N=0 is achieved with N_{max}=2 and the splittings obtained differ from those calculated with only N=0 by less than 1%. For the Stark effect, however, the Stark term itself mixes N=0 states with $N>0$. Terms off-diagonal in N are then very important and much larger basis sets are needed.

The scalar spin-spin interaction for N=0 is diagonal in the spin-coupled and fully coupled basis sets,

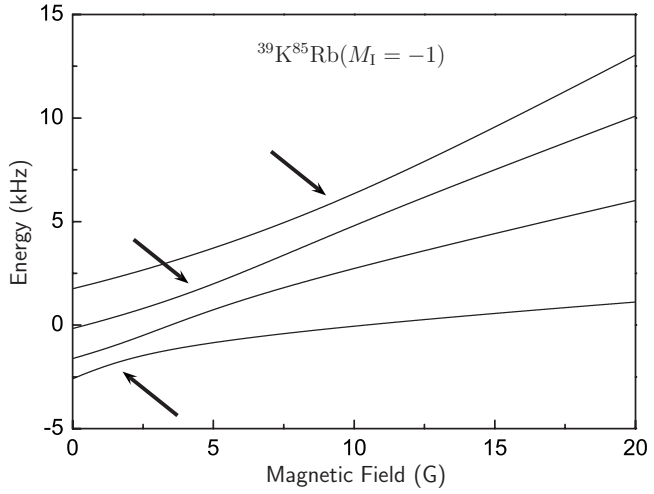

FIG. 2. Zeeman splitting and avoided crossings (indicated with arrows) for the M_I=−1 levels of ^{39}K^{85}Rb(v=0,N=0).

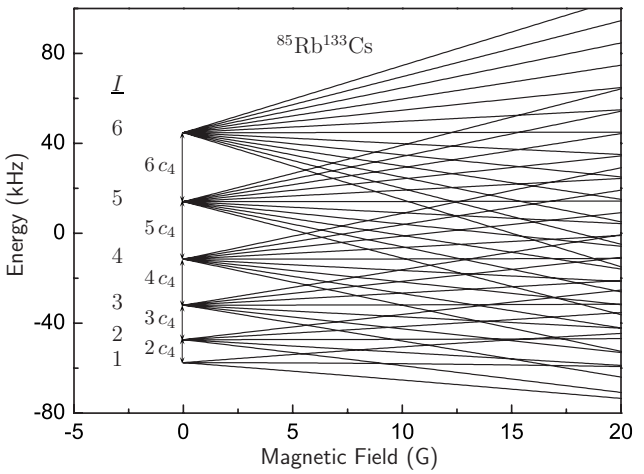

FIG. 3. Zeeman levels for ^{85}Rb^{133}Cs(v=0,N=0).

$$\begin{aligned}\langle N=0(I_1I_2)IM_I|c_4\boldsymbol{I}_1\cdot\boldsymbol{I}_2|N=0(I_1I_2)IM_I\rangle \\ =\langle N=0(I_1I_2)IFM_F|c_4\boldsymbol{I}_1\cdot\boldsymbol{I}_2|N=0(I_1I_2)IFM_F\rangle \\ =\frac{1}{2}c_4[I(I+1)-I_1(I_1+1)-I_2(I_2+1)].\end{aligned} \tag{13}$$

The nuclear Zeeman Hamiltonian is diagonal in the uncoupled basis set, with nonzero elements given by

$$-[g_1M_1(1-\sigma_1)+g_2M_2(1-\sigma_2)]\mu_N B. \tag{14}$$

The splitting pattern is therefore determined by the allowed values of the total nuclear spin quantum number I and by the magnitudes and signs of the scalar spin-spin coupling constant c_4 and the rotational g factors. The nuclear shielding constants σ_i are only a few parts per thousand. For large values of the magnetic field, where the nuclear Zeeman effect is the dominant term in the Hamiltonian, the magnetic moment (gradient of the energy with respect to B) is close to $-(g_1M_1+g_2M_2)\mu_N$.

The Zeeman splittings for ^{85}Rb^{133}Cs are shown in Fig. 3. They are qualitatively similar to those for ^{39}K^{85}Rb, except that the range of I is different and the spin-spin coupling constant c_4 is significantly larger. Because of this, I remains a good quantum number up to significantly higher magnetic fields. At high fields, once the magnitude of the scalar spin-spin interaction can be neglected compared to the Zeeman effect, M_{Rb} and M_{Cs} become good quantum numbers.

The splitting patterns for other KRb and RbCs isotopologs are qualitatively similar to those discussed above and the corresponding figures are available as supplementary online material [74]. The spin-spin coupling constant and the potassium g factor are negative for ^{40}K^{85}Rb and ^{40}K^{87}Rb. The sign of c_4 determines whether the lowest zero-field energy corresponds to the highest or lowest value of I. In general, the fields where the avoided crossings occur and above which M_1 and M_2 become good quantum numbers scale with $|c_4/(g_1-g_2)|$. When g_1 and g_2 are equal, as in homonuclear

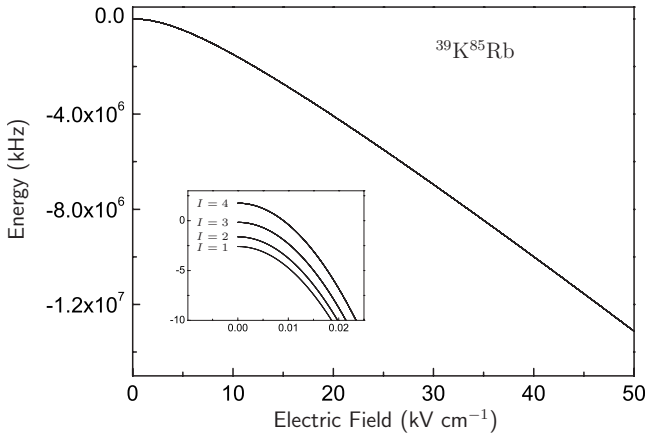

FIG. 4. Stark effect on energy levels of $^{39}K^{85}Rb$ correlating with (v=0, N=0) for electric fields up to 50 kV/cm.

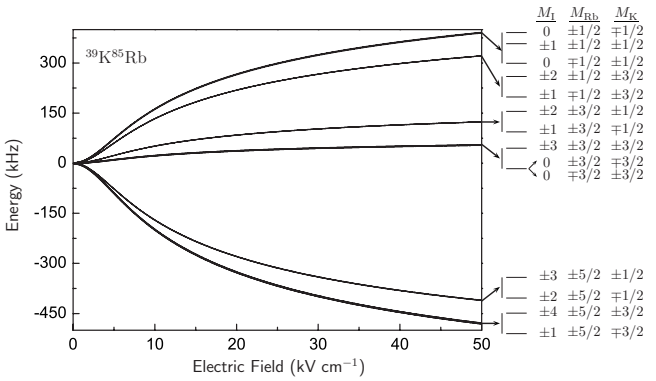

FIG. 6. Stark splitting for energy levels of $^{39}K^{85}Rb$ correlating with (v=0,N=0) for electric fields up to 50 kV/cm. The levels are shown relative to their field-dependent average energy.

dimers, there are no avoided crossings for N=0 and the I quantum number is conserved even at high fields.

B. Stark splitting for rotational ground-state molecules (N=0)

The Stark effect for levels of $^{39}K^{85}Rb$ correlating with N=0 is shown in Figs. 4–6. Corresponding figures for the remaining isotopologs of KRb and RbCs are available as additional online material [74]. The Stark effect is quadratic at low fields but becomes linear at high fields, as is usual for diatomic molecules in Σ states [75]. This arises from mixing between different rotational levels: while in the Zeeman case this mixing is very weak and is exclusively due to hyperfine terms, in the Stark case it is strong and is caused directly by the electric field. At low fields the mixing is weak and can be treated by second-order perturbation theory, giving rise to a quadratic Stark effect. However, as the field increases the mixing becomes increasingly important: the N=1 basis functions contribute around 25% at 10 kV/cm and 40% at 20 kV/cm. Eventually the molecule becomes fully oriented by the field and the linear Stark effect overcomes the quadratic effect. The mixing also has numerical consequences as the number of rotational levels required for convergence increases with field: for example, calculations at 50 kV/cm require N_{max}=6.

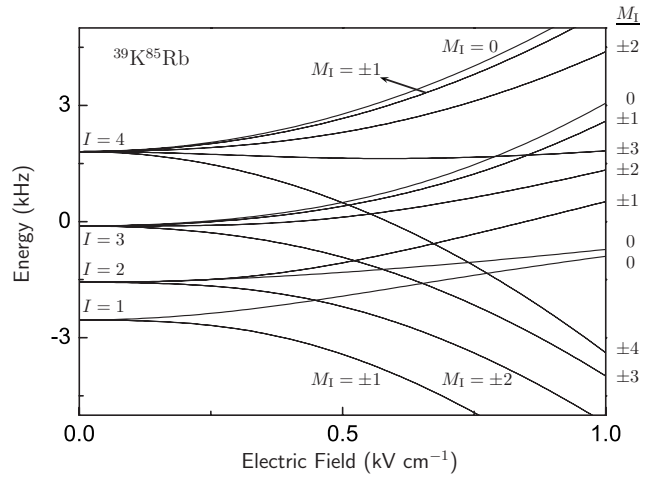

FIG. 5. Stark splitting for energy levels of $^{39}K^{85}Rb$ correlating with (v=0, N=0) for electric fields up to 1 kV/cm. The levels are shown relative to their field-dependent average energy.

The magnitude of the Stark shift in Fig. 4 obscures the splittings between hyperfine levels. Figure 5 therefore shows the levels correlating with N=0 relative to their average energy, for fields up to 1 kV/cm. As expected, each zero-field level splits into I+1 components labeled by the different possible values of $|M_I|$. For $|M_I|>0$ the levels exist in degenerate pairs corresponding to changing the sign of M_1 *and* M_2. However, changing the sign of *one* of M_1 and M_2 produces a different state with a different value of $|M_I|$. For M_I=0 there is an extra symmetry corresponding to reflection in a plane containing the electric field vector.

At higher field, as shown in Fig. 6, the projections of the individual nuclear spins become well defined as well as their sum. At sufficiently large fields the splittings approach a limiting value as the molecules become strongly oriented along the field direction. In this limit the splittings are mostly determined by the nuclear quadrupole coupling constants, with relatively small contributions from the magnetic hyperfine terms.

V. CONCLUSION

We have investigated the hyperfine level splittings expected for alkali-metal dimers in their rotational ground states in the presence of electric and magnetic fields. We have carried out density-functional calculations of the electronic structure of KRb and RbCs at the equilibrium geometry of the ground $^1\Sigma$ state and evaluated all the hyperfine coupling constants necessary to calculate energy level patterns. For nonrotating states, the zero-field splittings between hyperfine states range from a few kilohertz for isotopologs of KRb to a few tens of kilohertz for isotopologs of RbCs. They are dominated by the electron-mediated contribution to the nuclear spin-spin coupling. The results will be valuable in designing laser-based schemes to produce ultracold molecules in their absolute ground states in applied fields.

ACKNOWLEDGMENTS

The authors thank David J. Tozer and Michał Jaszuński for assistance and advice with the DFT calculations. We are grateful to EPSRC for funding of the collaborative project QuDipMol under the ESF EUROCORES Program EuroQUAM and to the U.K. National Centre for Computational Chemistry Software for computer facilities.

[1] J. M. Hutson and P. Soldán, Int. Rev. Phys. Chem. **25**, 497 (2006).
[2] K. M. Jones, E. Tiesinga, P. D. Lett, and P. S. Julienne, Rev. Mod. Phys. **78**, 483 (2006).
[3] T. Köhler, K. Goral, and P. S. Julienne, Rev. Mod. Phys. **78**, 1311 (2006).
[4] M. Baranov, Ł. Dobrek, K. Góral, L. Santos, and M. Lewenstein, Phys. Scr., T **102**, 74 (2002).
[5] D. DeMille, Phys. Rev. Lett. **88**, 067901 (2002).
[6] S. Jochim, M. Bartenstein, A. Altmeyer, G. Hendl, S. Riedl, C. Chin, J. H. Denschlag, and R. Grimm, Science **302**, 2101 (2003).
[7] M. W. Zwierlein, C. A. Stan, C. H. Schunck, S. M. F. Raupach, S. Gupta, Z. Hadzibabic, and W. Ketterle, Phys. Rev. Lett. **91**, 250401 (2003).
[8] M. Greiner, C. A. Regal, and D. S. Jin, Nature (London) **426**, 537 (2003).
[9] D. S. Petrov, C. Salomon, and G. V. Shlyapnikov, Phys. Rev. Lett. **93**, 090404 (2004).
[10] J. Herbig, T. Kraemer, M. Mark, T. Weber, C. Chin, H. C. Nägerl, and R. Grimm, Science **301**, 1510 (2003).
[11] P. Soldán, M. T. Cvitaš, J. M. Hutson, P. Honvault, and J. M. Launay, Phys. Rev. Lett. **89**, 153201 (2002).
[12] J. M. Hutson and P. Soldán, Int. Rev. Phys. Chem. **26**, 1 (2007).
[13] K. Winkler, F. Lang, G. Thalhammer, P. v. d. Straten, R. Grimm, and J. H. Denschlag, Phys. Rev. Lett. **98**, 043201 (2007).
[14] S. Ospelkaus, A. Pe'er, K.-K. Ni, J. J. Zirbel, B. Neyenhuis, S. Kotochigova, P. S. Julienne, J. Ye, and D. S. Jin, e-print arXiv:physics/0802.1093.
[15] J. G. Danzl, E. Haller, M. Gustavsson, M. J. Mark, R. Hart, N. Bouloufa, O. Dulieu, H. Ritsch, and H.-C. Nägerl, e-print arXiv:cond-mat/0806.2284.
[16] M. Mark, T. Kraemer, P. Waldburger, J. Herbig, C. Chin, H.-C. Nägerl, and R. Grimm, Phys. Rev. Lett. **99**, 113201 (2007).
[17] M. Mark, F. Ferlaino, S. Knoop, J. G. Danzl, T. Kraemer, C. Chin, H.-C. Nägerl, and R. Grimm, Phys. Rev. A **76**, 042514 (2007).
[18] C. Chin, V. Vuletić, A. J. Kerman, S. Chu, E. Tiesinga, P. J. Leo, and C. J. Williams, Phys. Rev. A **70**, 032701 (2004).
[19] J. M. Hutson, E. Tiesinga, and P. S. Julienne, e-print arXiv:physics/0806.2583, Phys. Rev. A (to be published).
[20] N. F. Ramsey, Phys. Rev. **85**, 60 (1952).
[21] J. M. Brown and A. Carrington, *Rotational Spectroscopy of Diatomic Molecules* (Cambridge University Press, Cambridge, U.K., 2003).
[22] D. L. Bryce and R. E. Wasylishen, Acc. Chem. Res. **36**, 327 (2003).
[23] N. J. Stone, At. Data Nucl. Data Tables **90**, 75 (2005).
[24] S. Kotochigova, P. S. Julienne, and E. Tiesinga, Phys. Rev. A **68**, 022501 (2003).
[25] S. Kotochigova and E. Tiesinga, J. Chem. Phys. **123**, 174304 (2005).
[26] P. E. Van Esbroeck, R. A. McLean, T. D. Gaily, R. A. Holt, and S. D. Rosner, Phys. Rev. A **32**, 2595 (1985).
[27] R. A. Logan, R. E. Coté, and P. Kusch, Phys. Rev. **86**, 280 (1952).
[28] P. A. Bonczyk and V. W. Hughes, Phys. Rev. **161**, 15 (1967).
[29] P. J. Dagdigian and L. Wharton, J. Chem. Phys. **57**, 1487 (1972).
[30] J. Cederberg, E. Frodermann, H. Tollerud, K. Huber, M. Bongard, J. Randolph, and D. Nitz, J. Chem. Phys. **124**, 244304 (2006).
[31] J. Cederberg, S. Fortman, B. Porter, M. Etten, M. Feig, M. Bongard, and L. Langer, J. Chem. Phys. **124**, 244305 (2006).
[32] E. Tiemann, B. Holzer, and J. Hoeft, Z. Naturforsch. A **32**, 123 (1977).
[33] E. Tiemann, B. Holzer, and J. Hoeft, Z. Naturforsch. A **31**, 236 (1976).
[34] J. Cederberg, J. Ward, G. McAlister, G. Hilk, E. Beall, and D. Olson, J. Chem. Phys. **111**, 8396 (1999).
[35] J. Hoeft, E. Tiemann, and T. Torring, Z. Naturforsch. A **27**, 1516 (1972).
[36] T. Helgaker, M. Jaszuński, and K. Ruud, Chem. Rev. (Washington, D.C.) **99**, 293 (1999).
[37] G. te Velde, F. M. Bickelhaupt, S. J. A. van Gisbergen, C. Fonseca Guerra, E. J. Baerends, J. G. Snijders, and T. Ziegler, J. Comput. Chem. **22**, 931 (2001).
[38] Computer code ADF2007.01, SCM, Theoretical Chemistry, Vrije Universiteit, Amsterdam, The Netherlands, http://www.scm.com.
[39] Computer code DALTON release 2.0, http://www.kjemi.uio.no/software/dalton/dalton.html.
[40] R. A. Brooks, C. H. Anderson, and N. F. Ramsey, Phys. Rev. Lett. **10**, 441 (1963).
[41] R. A. Brooks, C. H. Anderson, and N. F. Ramsey, J. Chem. Phys. **56**, 5193 (1972).
[42] E. van Lenthe, E. J. Baerends, and J. G. Snijders, J. Chem. Phys. **99**, 4597 (1993).
[43] E. van Lenthe, E. J. Baerends, and J. G. Snijders, J. Chem. Phys. **101**, 9783 (1994).
[44] E. van Lenthe, E. J. Baerends, and J. G. Snijders, J. Chem. Phys. **110**, 8943 (1999).
[45] O. L. Fedotov, M. A. Malkina, and V. G. Malkin, Chem. Phys. Lett. **258**, 330 (1996).
[46] W. C. Bailey, J. Mol. Spectrosc. **190**, 318 (1998).
[47] W. C. Bailey, Chem. Phys. Lett. **292**, 71 (1998).
[48] W. C. Bailey, Chem. Phys. **252**, 57 (2000).
[49] E. van Lenthe and E. J. Baerends, J. Chem. Phys. **112**, 8279 (2000).
[50] I. Hung and R. W. Schurko, Solid State Nucl. Magn. Reson.

24, 78 (2003).
[51] M. H. Palmer and A. D. Nelson, J. Mol. Struct. **828**, 91 (2007).
[52] F. A. Bischoff, O. Hübner, W. Klopper, L. Schnelzer, B. Pilawa, M. Horvatić, and C. Berthier, Eur. Phys. J. B **55**, 229 (2007).
[53] H. Behzadi, N. L. Hadipour, and M. Mirzaei, Biophys. Chem. **125**, 179 (2007).
[54] C. Lee, W. Yang, and R. G. Parr, Phys. Rev. B **37**, 785 (1988).
[55] A. D. Becke, J. Chem. Phys. **98**, 5648 (1993).
[56] T. W. Keal and D. J. Tozer, J. Chem. Phys. **119**, 3015 (2003).
[57] T. W. Keal, D. J. Tozer, and T. Helgaker, Chem. Phys. Lett. **391**, 374 (2004).
[58] A. D. Becke, Phys. Rev. A **38**, 3098 (1988).
[59] J. Vaara, J. Jokisaari, R. E. Wasylishen, and D. L. Bryce, Prog. Nucl. Magn. Reson. Spectrosc. **41**, 233 (2002).
[60] T. Helgaker, M. Jaszuński, and M. Pecul, Prog. Nucl. Magn. Reson. Spectrosc. **53**(4), 249 (2008).
[61] J. P. Perdew, K. Burke, and M. Ernzerhof, Phys. Rev. Lett. **77**, 3865 (1996).
[62] W. H. Flygare, J. Chem. Phys. **41**, 793 (1964).
[63] T. D. Gierke and W. H. Flygare, J. Am. Chem. Soc. **94**, 7277 (1972).
[64] R. E. Wasylishen, D. L. Bryce, C. J. Evans, and M. C. L. Gerry, J. Mol. Spectrosc. **204**, 184 (2000).
[65] S. A. Cooke and M. C. L. Gerry, Phys. Chem. Chem. Phys. **6**, 4579 (2004).
[66] S. Huzinaga and B. Miguel, Chem. Phys. Lett. **175**, 289 (1990).
[67] S. Huzinaga and M. Klobukowski, Chem. Phys. Lett. **212**, 260 (1993).
[68] D. J. D. Wilson, C. E. Mohn, and T. Helgaker, J. Chem. Theory Comput. **1**, 877 (2005).
[69] T. Enevoldsen, T. Rasmussen, and S. P. A. Sauer, J. Chem. Phys. **114**, 84 (2001).
[70] A. J. Ross, C. Effantin, P. Crozet, and E. Boursey, J. Phys. B **23**, L247 (1990).
[71] H. Katô and H. Kobayashi, J. Chem. Phys. **79**, 123 (1983).
[72] T. R. Lawrence, C. H. Anderson, and N. F. Ramsey, Phys. Rev. **130**, 1865 (1963).
[73] R. N. Zare, *Angular Momentum* (John Wiley & Sons, New York, 1987).
[74] See EPAPS Document No. E-PLRAAN-78-170809 for the splitting patterns corresponding to the KRb and RbCs isotopologs not included in the paper. For more information on EPAPS, see http://www.aip.org/pubservs/epaps.html.
[75] R. N. Townes and A. L. Schawlow, *Microwave Spectroscopy* (Dover, New York, 1975).